



## Geothermal power potential at the western coastal part of Saudi Arabia



Mohamed T. Hussein<sup>a,c</sup>, Aref Lashin<sup>a,b,\*</sup>, Abdulaziz Al Bassam<sup>a,c</sup>, Nassir Al Arifi<sup>a</sup>, Ibrahim Al Zahrani<sup>d</sup>

<sup>a</sup> King Saud University, College of Science, Geology and Geophysics Department, P.O. Box 2455, Riyadh 11451, Saudi Arabia

<sup>b</sup> Benha University, Faculty of Science, Geology Department, P. O. Box 13518, Benha, Egypt

<sup>c</sup> Saudi Geological Survey Research Chair (SGSRC), King Saud University, Saudi Arabia

<sup>d</sup> Saudi Geological Survey (SGS), Jeddah, Saudi Arabia

### ARTICLE INFO

#### Article history:

Received 8 November 2012

Received in revised form

6 May 2013

Accepted 20 May 2013

Available online 10 July 2013

#### Keywords:

Geothermal energy

Surface lineation

2D electric profiles

Reserve estimation

Wadi Al-Lith

### ABSTRACT

Saudi Arabia is enriched by many geothermal resources that are located along the western coastal part of the Red Sea, in the form of a number of hot springs and many volcanic eruptions. Wadi Al-Lith is considered one of the most promising geothermal targets that encounter many hot springs with a good surface temperature upto 95 °C. This paper aims mainly to evaluate the geothermal potential of the main hot spring at Wadi Al-Lith area (Ain Al Harrah). The available remote sensing images are analyzed and a number of 2D electric resistivity profiles are interpreted to delineate the surface geological lineaments and the subsurface structural elements that control the movement of the thermal water. It is found that the main surface lineaments are structurally oriented along NNE–SSW and NE–SW directions with a frequency percentage of 52% and an average lineament length of 835 m. Furthermore the subsurface structural elements, as inferred from the interpretation of the geophysical 2D electric profiles, have assumed the same directions beside the NW–SE direction.

The characteristics of thermal water of the hot spring are indicated through analyzing the major and minor elements of some collected water samples. Geo-thermometers are applied to estimate, subsurface temperature, heat flow and discharge enthalpy. These parameters are found to be 136 °C, 183 mW/M<sup>2</sup> and 219 kJ/kg, respectively. An estimate of the geothermal reserve using the volumetric method, gave total stored heat energy of  $1.713 \times 10^{17}$  J (rock and fluid) and a geothermal reserve potential of 26.99 MWt.

It appears from our research that the estimated energy is quite enough for operating a medium scale power plant that utilizes low boiling point fluid (Kalina Cycle) for limited electricity production, beside other low-temperature applications (district heating, green houses and medical therapy).

© 2013 Elsevier Ltd. Open access under CC BY-NC-SA license.

### Contents

1. Introduction . . . . .	669
2. Geologic setting . . . . .	669
2.1. Rock units . . . . .	669
2.2. Topography . . . . .	672
3. Methodology . . . . .	673
3.1. Landsat RGB images . . . . .	673
3.1.1. Gridding and mapping of lineation . . . . .	673
3.2. Geophysical surveys . . . . .	677
3.3. Petro-thermal characteristics of thermal water . . . . .	677
3.3.1. Geo-thermometers . . . . .	678
3.3.2. Ternary diagrams . . . . .	679
3.4. Geothermal reserve estimation . . . . .	679

\* Corresponding author at: King Saud University, College of Science, Geology and Geophysics Department, P. O. Box 2455, Riyadh 11451, Saudi Arabia.

Tel.: +966 540852336; fax: +966 14670389.

E-mail addresses: [aref70@hotmail.com](mailto:aref70@hotmail.com), [alashin@ksu.edu.sa](mailto:alashin@ksu.edu.sa) (A. Lashin).

4. Results and discussion.....	680
4.1. Lineaments extraction and analysis .....	680
4.2. Interpretation of geophysical profiles.....	680
4.3. Characteristics of thermal water.....	682
4.4. Geothermal energy potential .....	682
4.4.1. Utilization of geothermal energy in Saudi Arabia and economic and social impact.....	682
5. Conclusions .....	683
Acknowledgments.....	683
References .....	683

## 1. Introduction

Geothermal power is among the renewable energy sources which come from natural resources such as sunlight, wind, rain, tides, and biomass which are renewable. About 16% of global final energy consumption comes from renewables, with 10% coming from traditional biomass, which is mainly used for heating, and 3.4% from hydroelectricity. New renewables (small hydro, modern biomass, wind, solar, geothermal, and biofuels) accounted for another 3% and are growing very rapidly. The share of renewables in electricity generation is around 19%, with 16% of global electricity coming from hydroelectricity and 3% from new renewables [1,2].

The most critical factor for the classification of geothermal energy as a renewable energy scale is the rate of energy recharge. In the exploitation of natural geothermal systems, energy recharge takes place by advection of thermal water on the same time scale as production from the resource. This justifies our classification of geothermal energy as a renewable energy resource. In the case of hot, dry rocks, and some of the hot water aquifers in sedimentary basins, energy recharge is only by thermal conduction; due to the slow rate of the latter process, however, hot dry rocks and some sedimentary reservoirs should be considered as finite energy resources [3].

Geothermal power is cost effective, reliable, sustainable, and environmentally friendly, but has historically been limited to areas near tectonic plate boundaries. Recent technological advances have dramatically expanded the range and size of viable resources, especially for applications such as home heating, opening a potential for widespread exploitation. Geothermal wells release greenhouse gases trapped deep within the earth, but these emissions are much lower per energy unit than those of fossil fuels. The International Geothermal Association (IGA) has reported that 10,715 MW of the online geothermal power in 24 countries, are generating 67,246 GWh of electricity in 2010. This represented a 20% increase in geothermal power online capacity since 2005. IGA expects that this will grow to 18,500 MW by 2015, due to the large number of projects presently under consideration, often in areas previously assumed to have little exploitable resource [4,5].

In Saudi Arabia there is a big gap of knowledge and information concerning the potential of geothermal resources. A more detailed and much more comprehensive work is needed to study the geothermal resources in Saudi Arabia, especially those encountered in Southwestern parts, from one hand, and to evaluate their economic reserves for possible energy production and domestic application, from the other hand. Large number of exploration methods and technologies should be initiated in order to reach these objectives. Many of these methods are in current use and have already been widely experimented in other sectors of research [6].

The geothermal resources of Saudi Arabia can be categorized as the following:

1. *Low enthalpy resources (sedimentary aquifers)*: represented by deep-seated aquifers encountered in thick sedimentary basins in the eastern part of the Kingdom. These resources are

confined and geothermal potential is represented by the normal geothermal gradient. It can be accessed only by deep drilled wells (i.e. oil wells).

2. *Medium enthalpy resources (hot springs)*: encountered along the western and southwestern coastal parts and represented by the shallow hot springs of hot surface water. These resources are unconfined targets with direct accesses to the subsurface hot anomalies through an open network of active faults and fractures (structure control).
3. *High enthalpy resources (basaltic lavas, Harrats)*: Saudi Arabia has approximately 80,000 km<sup>2</sup> of lava fields, known as Harrats. They are represented by volcanic eruptions, mainly basaltic in composition, that extend along the coastal part of the Red Sea at the western of Saudi Arabia. Harrats of Khaybar and Rahat are believed to be the best in terms of high heat flow and enthalpy [6].

The first geothermal work done at Saudi Arabia was that of El Dayel, 1988 [7]. He focused mainly on studying the hydro-chemical characteristics of the hot springs at Jizan and Al-Lith areas. Some water samples from the hot springs were analyzed. Other interested work regarding the petrography, petrochemical composition and mineralogy of the basaltic volcanic eruptions, was done by Roobol et al. and Pint et al. in the period from 1992 to 2007. A more detailed and recent work is done by Lashin and Al Arifi, 2012 [8]. They focused on giving a preliminary investigation of the geothermal resources encountered in the southwestern parts of the Saudi Arabia (Jizan area), based on the interpretations of the Landsat images and chemical analyses.

In general, a few studies have presented the characteristics and the potentiality of the geothermal resources and its utility for some locations along the western coastal area of Red Sea of Saudi Arabia [8–14]. This work presents an initial evaluation of the geothermal energy potential of Wadi Al-Lith area, and provides a basis for a preliminary assessment of geothermal resources in the whole region.

## 2. Geologic setting

### 2.1. Rock units

Wadi Al-Lith is represented by a catchment area that is considered an integral part of the Arabian Shield. It extends from the western coast of the Red Sea to high Mountains in the east. The area is mainly covered by metavolcanic rocks, metasediments and late Proterozoic plutonic rocks (Fig. 1). Four major rock units are found covering about 91% of Wadi Al-Lith catchment area. These rock units are summarized, from youngest to oldest, as follows:

- 1- *Quaternary, sand, gravel and silt*: This unit represents 18% of the total catchment area of Wadi Al-Lith. Eolian sand-dune fields,

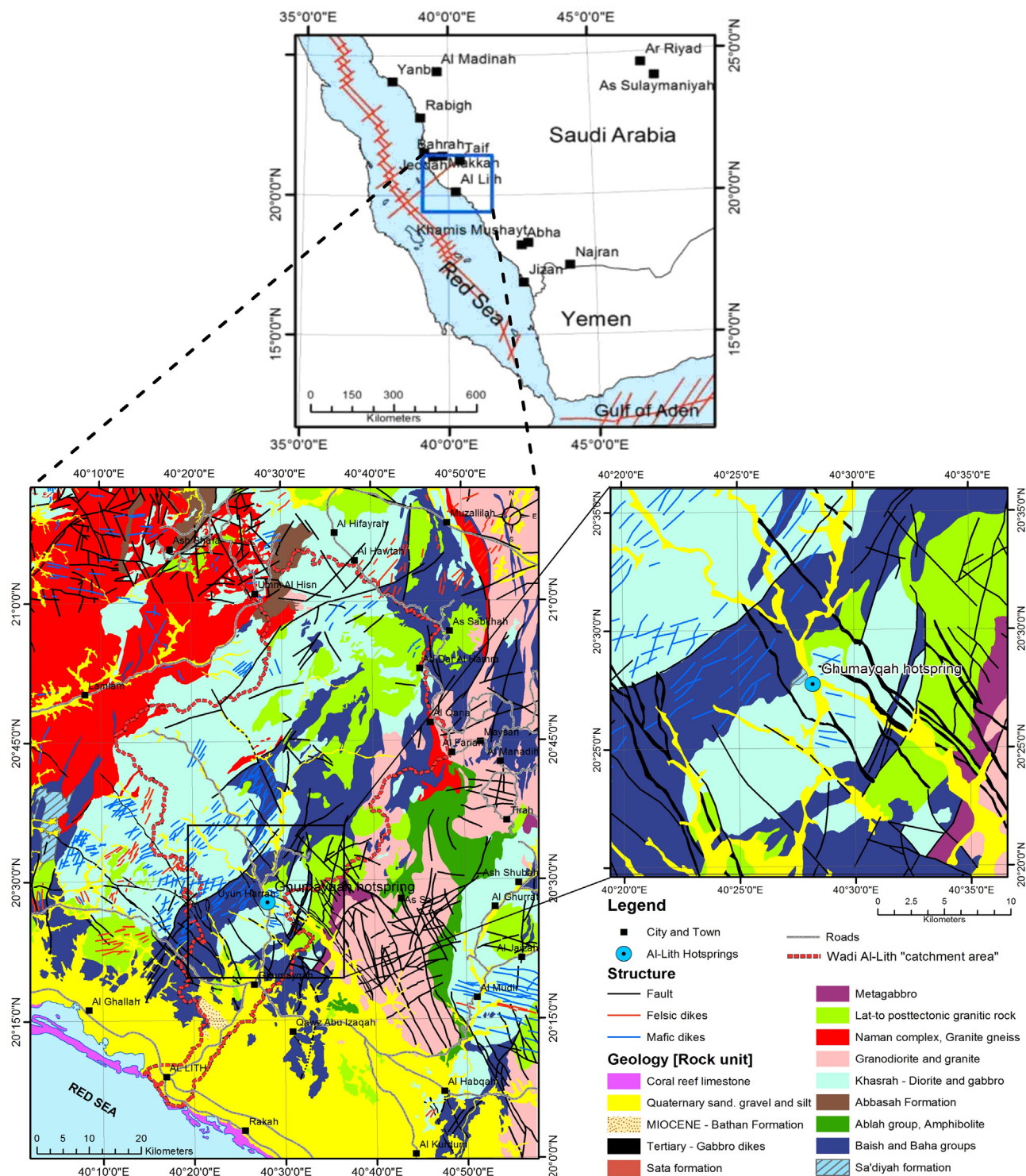


Fig. 1. Geologic map of Wadi Al-Lith area showing Ain Al Harrah hot spring.

mobile sheet sand and silt deposits cover a large proportion of the coastal plain in the southern part of the study area. Barrier, longitudinal, and barchans dunes are present locally, and most of the area is covered by sand deposits.

- 2- *Late- to post-tectonic granitic rocks*: These rocks are part of the Proterozoic intrusive rocks that cover most of the western part of the study area. They represent 13% of the total basin area of Wadi Al-Lith. The plutonic rocks range in composition from

serpentinite to syenite, although diorite, tonalite, granodiorite, and monzogranite predominate.

- 3- *Lith suite, Khasrah complex, diorite and gabbro*: These rocks contain mafic to intermediate plutonic rocks that crops out in a wide northeast trending belt in the western part of Wadi Al-Lith basin. It covers almost 37% from Wadi Al-Lith basin area.
- 4- *Baish and Baha groups*: Many rocks assigned to the undivided Baish and Bahah groups crops out in the eastern part of Wadi



Al-Lith basin as “basalt and dacite”, and “biotite-hornblende schist, and amphibolite” covering almost 23% from Wadi Al-Lith basin area.

Other rock units are found constituting about 9% of wadi Al-Lith basin. The most important of these rocks are the metagabbro, gabbro dikes, syntectonic granitic rock, granodiorite, granite and amphibolite, as shown on the geological map (Fig. 1).

The main structural elements which are prevailing along the western coastal part (Red Sea) of the Saudi Arabia, including the study area, can be classified as:

- Precambrian northwest–southeast to east–west compression that are reactivated by tensional stress field during the Tertiary evolution of the Red Sea rift.
- Tertiary northeast–southwest tension.

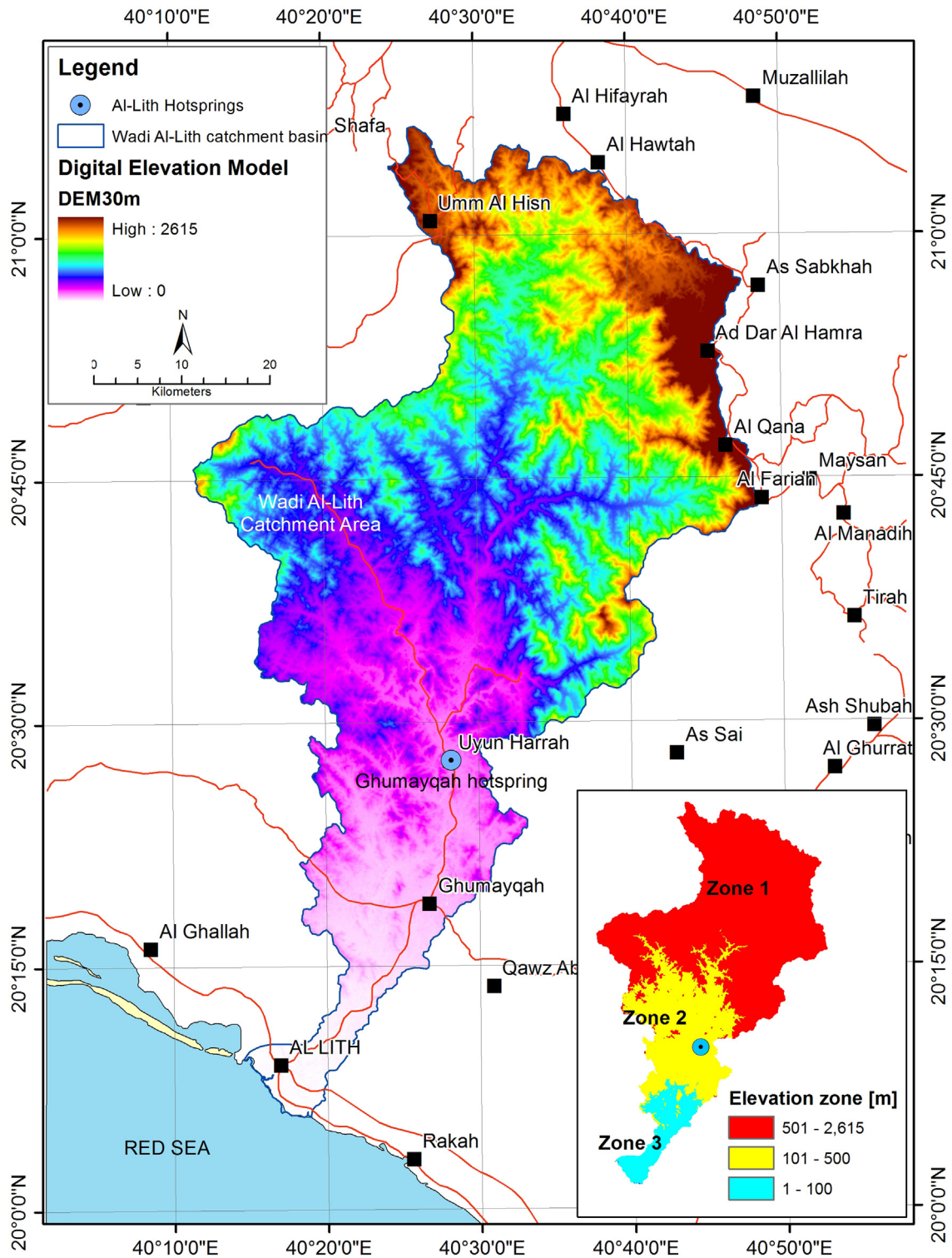


Fig. 2. Digital elevation model of Wadi Al-Lith basin.



These structural elements are believed to be the main channels and pathways through which the thermal water rises to the surface.

## 2.2. Topography

Fig. 2 exhibits the digital elevation model of Wadi Al-Lith basin, which shows a wide variation in the topography of the area. A maximum depth of 2600 m (above sea level) is recorded at the highly elevated mountainous area in the northern part of Wadi

Al-Lith basin, while an elevation of less than 1 m is recorded for the sea-ward coastal plains in the southern part of the area.

According to its surface elevation from the sea level, Wadi Al-Lith basin can be divided into three zones, as follows:

- 1- A high mountainous upstream zone: the elevation ranges from 500 m to 2600 m above the sea level and is characterized by high degrees of slopes and rugged area. It includes a number of tributaries and sub-wadies such as; Wadi Birayn, Wadi

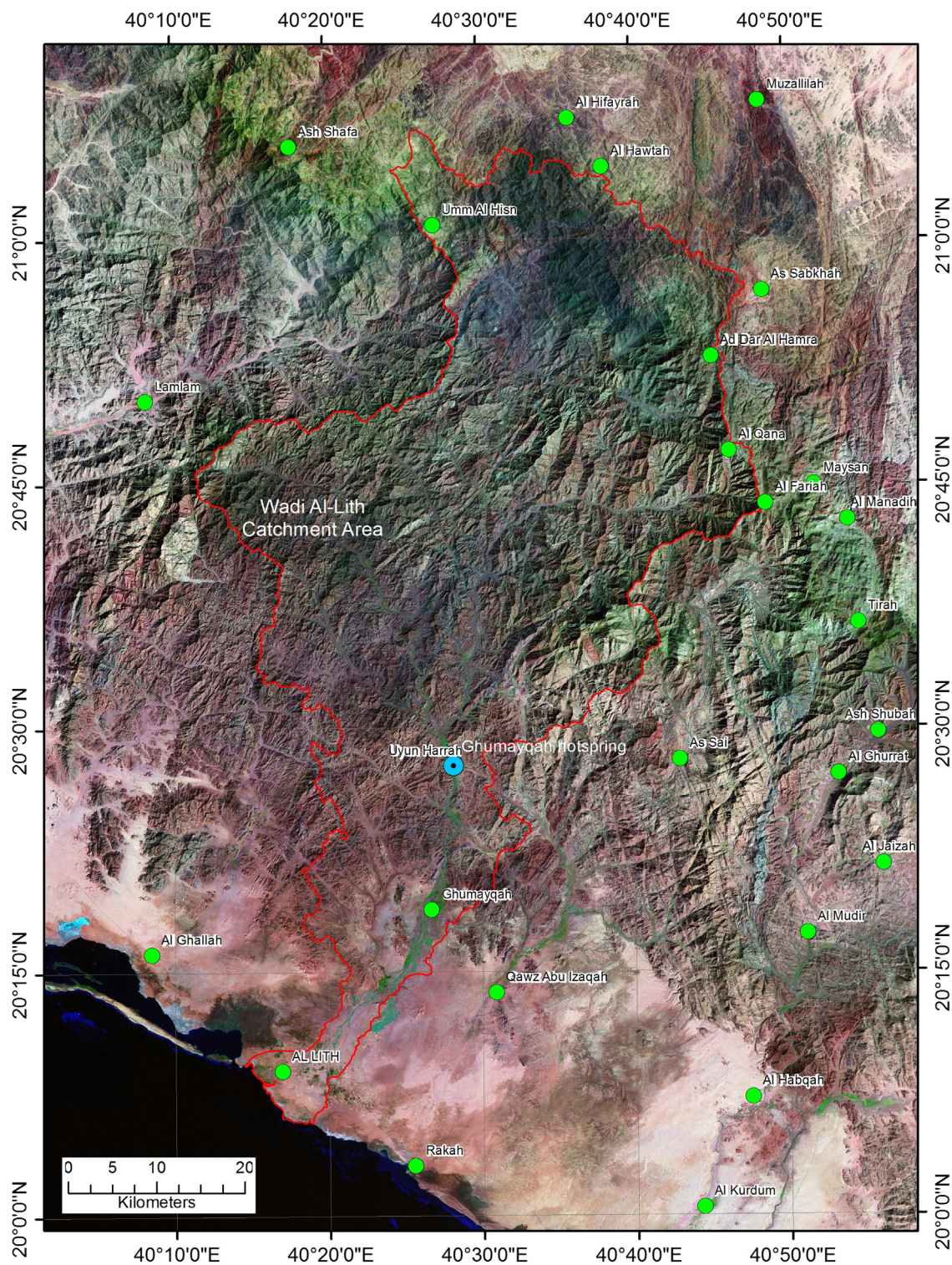


Fig. 3. Landsat RGB image of Wadi Al-Lith catchment area.



- 2- An intermediate zone of small hills and mountains: the elevation of this zone ranges from 100 m to 500 m above sea level. It represents the midstream of the Wadi Al-Lith and includes the main tributaries and wadies sloping from up-stream. It is characterized by moderate gradient and encounters the major waterways of the Wadi Al-Lith.
- 3- The coastal flood plain down-stream zone: this zone contains alluvial deposits with an elevation range from 100 m to nearly zero at the shoreline of the Red Sea.

Locality Name & No.	Wadi Al-Lith 28	Sampling date	28 May 2011			TDS	1127 ppm		
Longitude	20°17'32.11	Type of aquifer	Water well			PH	7.5		
Latitude	40°28'36.11	Temperature	34 °C			EC	1879 μS cm <sup>-1</sup>		
		Elevation	60.0 m						
Chemical composition (mg/l)									
SiO <sub>2</sub>	Na <sup>+</sup>	K <sup>+</sup>	Ca <sup>++</sup>	Mg <sup>++</sup>	SO <sub>4</sub> <sup>--</sup>	NH <sub>4</sub>	HCO <sub>3</sub> <sup>-</sup>	Cl <sup>-</sup>	F <sup>-</sup>
39.28	212.6	9.34	103	37.8	340		38.872	185.9	0.61
Chemical composition (10 <sup>-3</sup> mg/l)									
Li	Al	Zn	Fe	Cu	Mn	Ni	Co	Ba	B
1.68	9.21	2.93	270	1.91	0.638	4.06	0.294	27.4	505
Chemical composition (ppb)									
Rb	Cr	V	Mo	Sr	U	Th	Not detected		
0.587	56.8	41	23.2	1630	2.6		Over range		

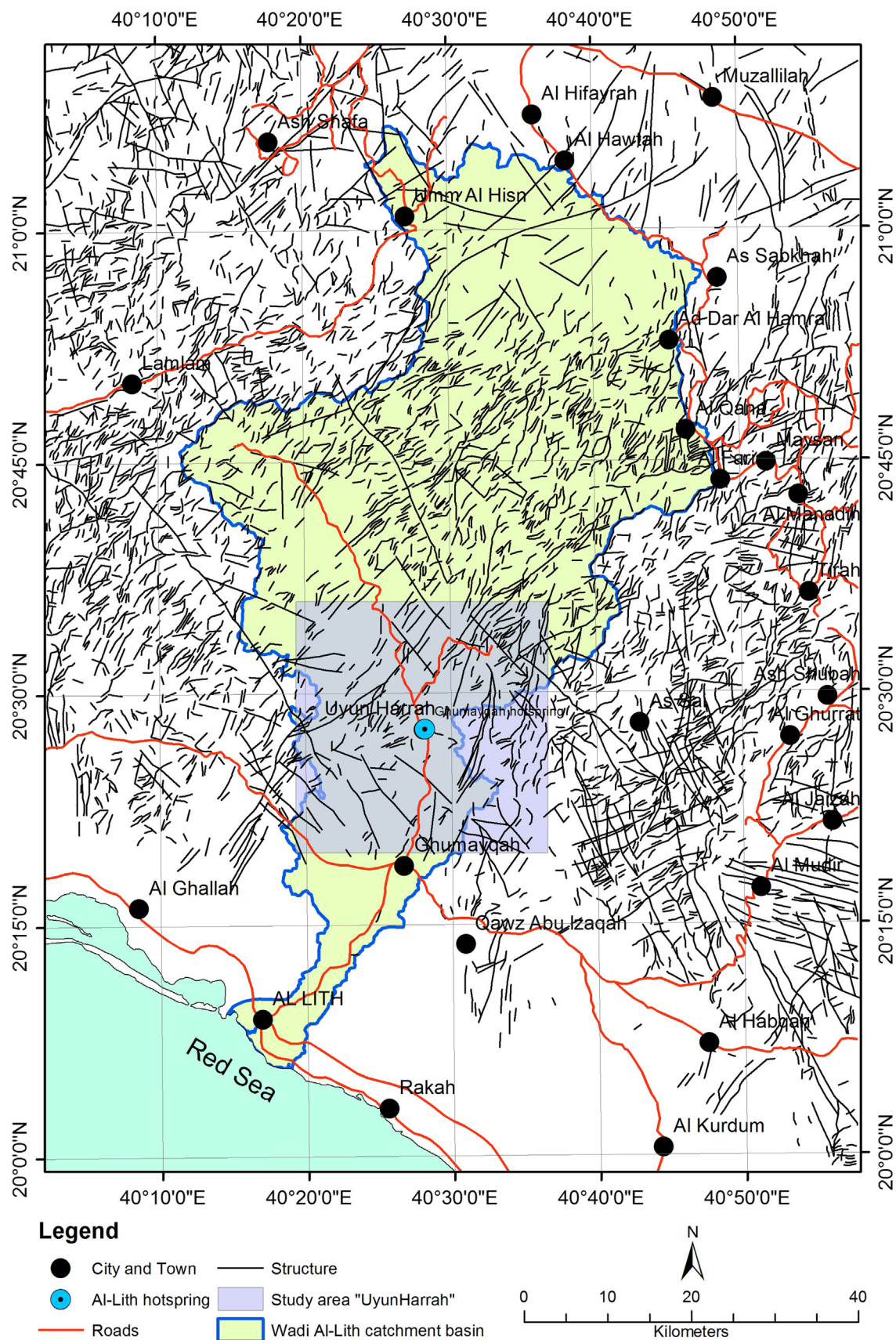


Fig. 4. Interpretation of the lineaments of Wadi Al-Lith area as extracted from the analysis of the Landsat GRB image.



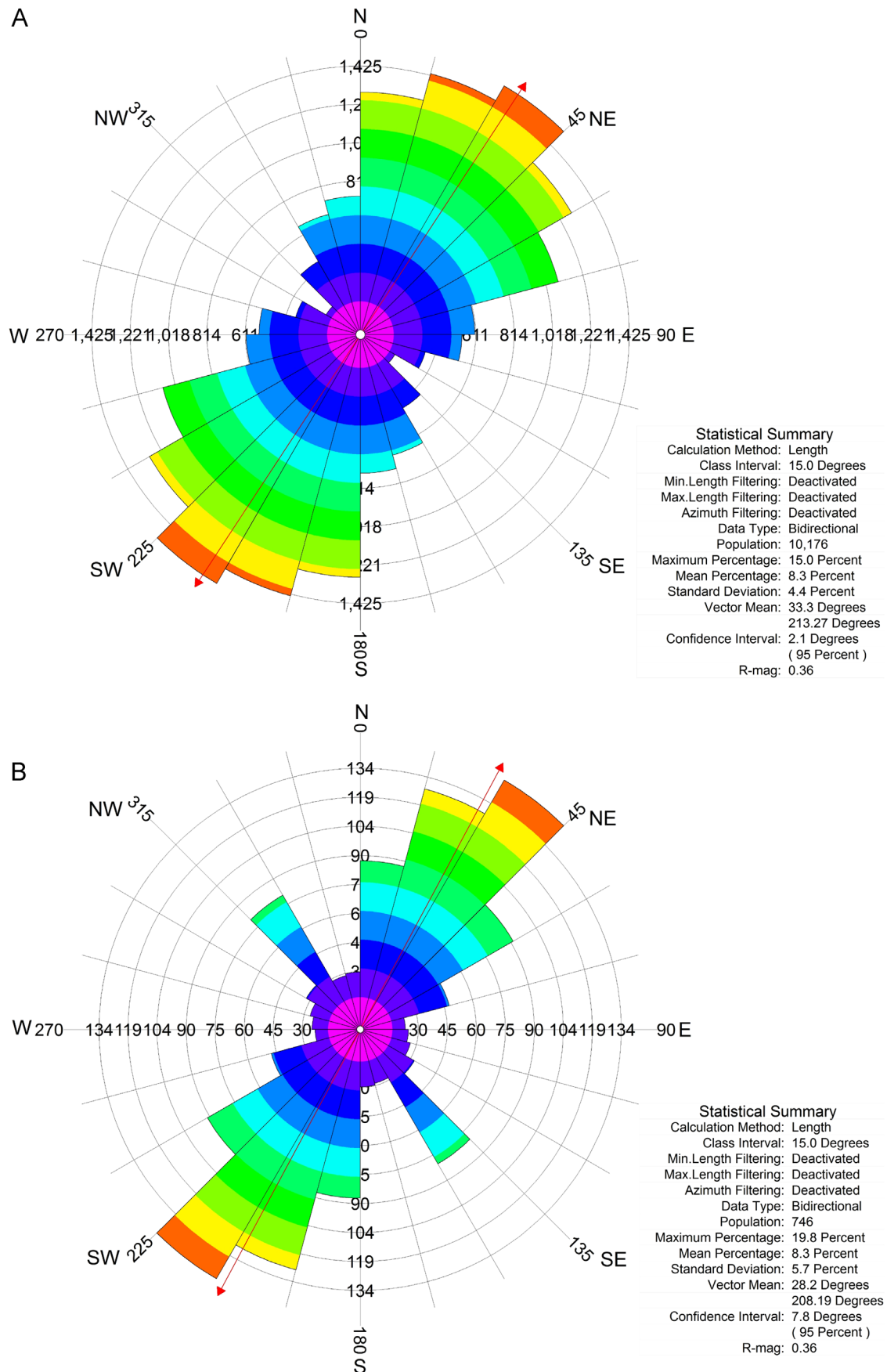


Fig. 5. Rose diagram showing the structure lineaments of (A) Wadi Al-Lith area and (B) Ain Al Harrah hot spring area.

**Table 3**

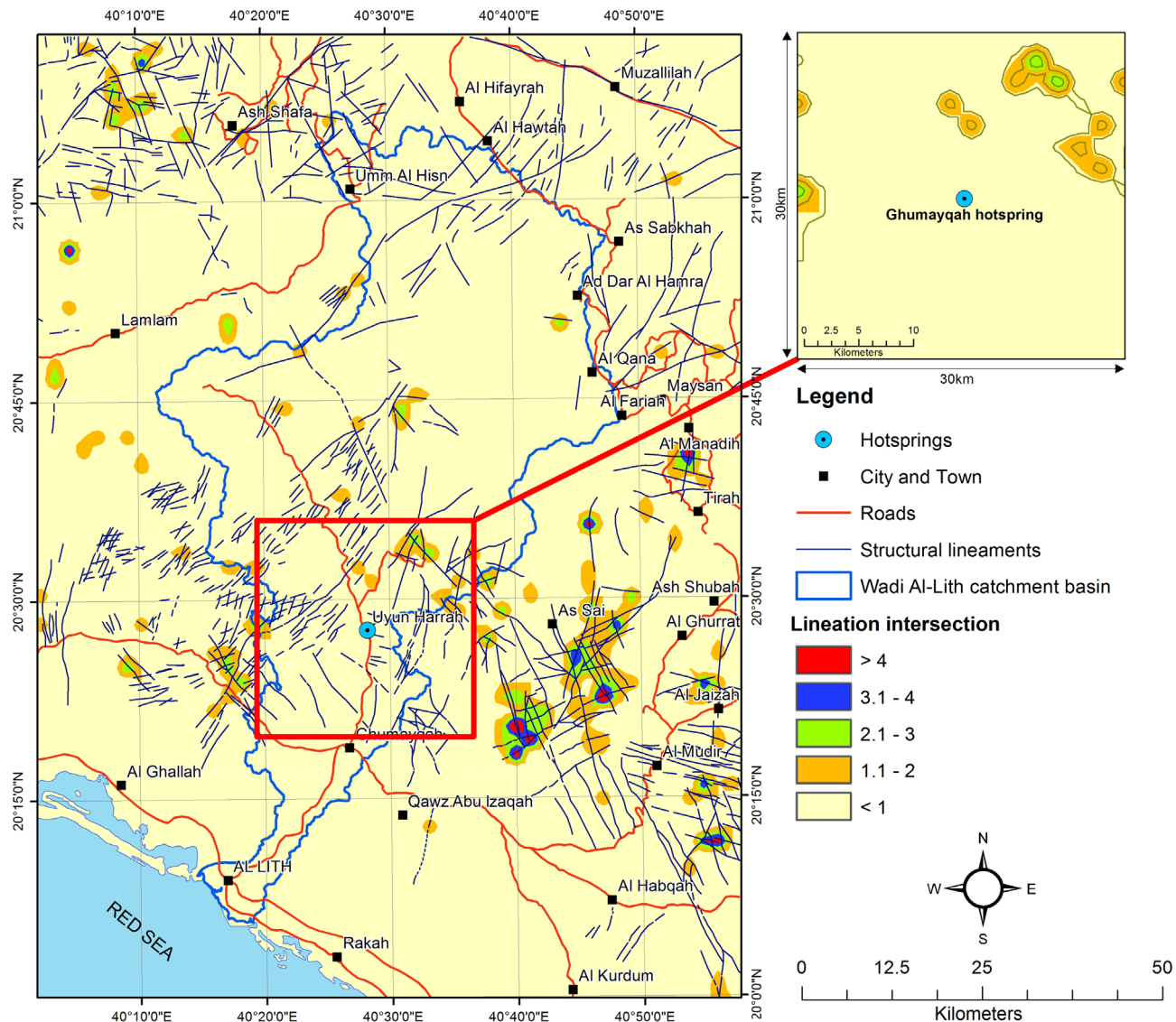
The directional trends of the extracted lineaments in the Wadi Al-Lith area.

Lineaments structure trend	Degrees range	Frequencies	Percent	Avg. length (m)	SD
N-S	(0–11.25), (168.75–191.25) and (348.75–360)	1644	16.2	759	569
NNE-SSW	(11.25–33.75) and (191.25–213.75)	2297	22.6	745	488
NE-SW	(33.75–56.25) and (213.75–236.25)	2230	21.9	764	535
ENE-WSW	(56.25–78.75) and (236.25–258.75)	1683	16.5	757	619
E-W	(78.75–101.25) and (258.75–281.25)	839	8.2	777	699
ESE-WNW	(101.25–123.75) and (281.25–303.75)	329	3.2	1287	1153
SE-NW	(123.75–146.25) and (303.75–326.25)	339	3.3	1095	827
SSE-NNW	(146.25–168.75) and (326.25–348.75)	815	8.0	968	676

**Table 4**

The directional trends of the extracted lineaments of Ain Al Harrah area.

Lineaments structure trend	Degrees range	Frequencies	Percent	Avg. length (m)	SD
N-S	(0–11.25), (168.75–191.25) and (348.75–360)	99	13.3	803	528
NNE-SSW	(11.25–33.75) and (191.25–213.75)	193	25.9	822	613
NE-SW	(33.75–56.25) and (213.75–236.25)	195	26.1	847	644
ENE-WSW	(56.25–78.75) and (236.25–258.75)	97	13.0	687	435
E-W	(78.75–101.25) and (258.75–281.25)	33	4.4	922	757
ESE-WNW	(101.25–123.75) and (281.25–303.75)	24	3.2	164	83
SE-NW	(123.75–146.25) and (303.75–326.25)	61	8.2	154	54
SSE-NNW	(146.25–168.75) and (326.25–348.75)	44	5.9	214	89

**Fig. 6.** Lineation intersection grid map of Wadi Al-Lith basin including Ain Al Harrah area.

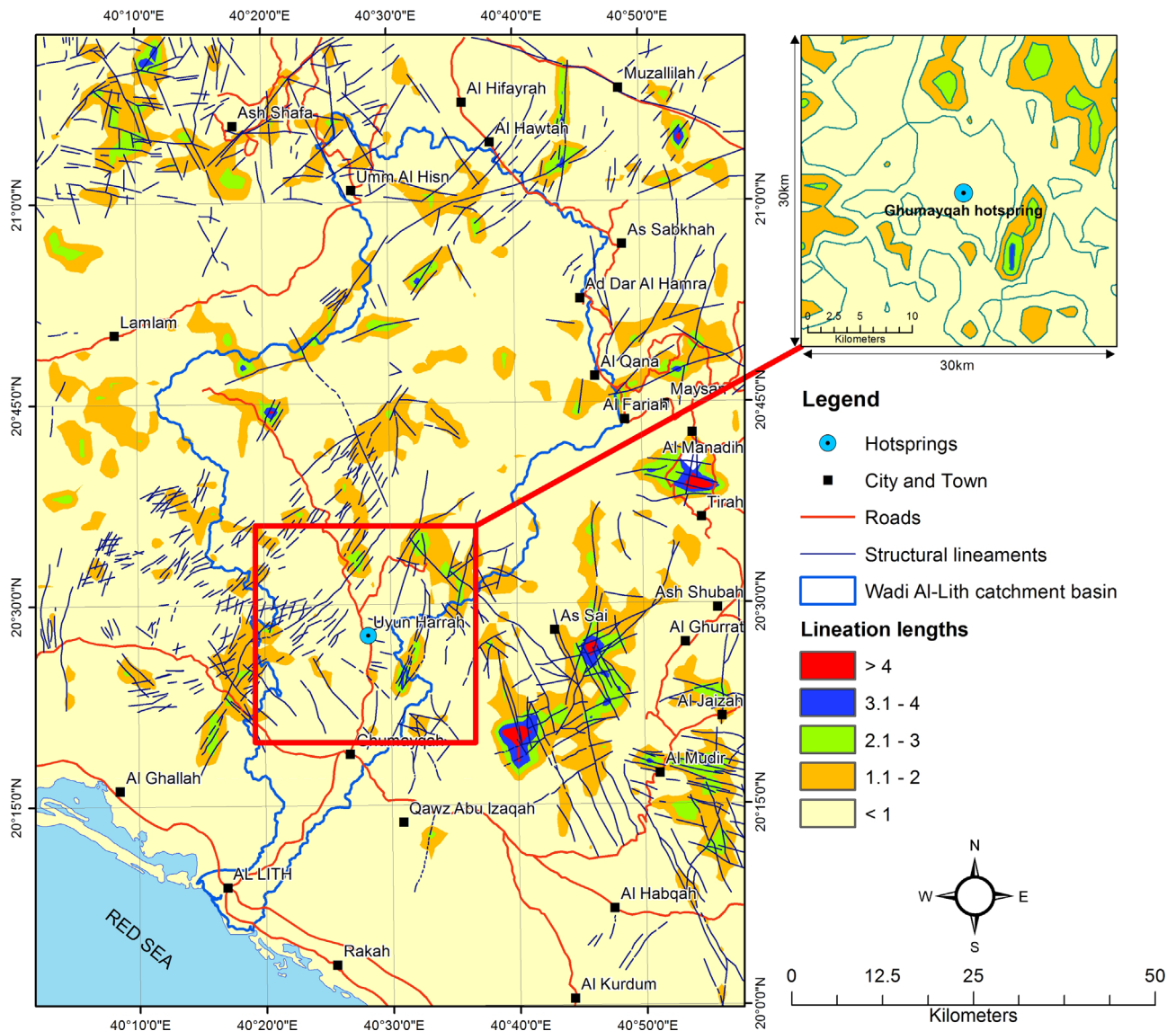


Fig. 7. Lineation length grid map of Wadi Al-Lith basin including Ain Al Harrah area.

geothermal targets and detecting their possible lateral extension as well as the structural elements which may control the subsurface movement of the arising geothermal water.

### 3.2. Geophysical surveys

The geothermal potential can be explored and investigated using a variety of geophysical and geochemical (geo-thermometers) techniques which are normally used in geo-technical and geological investigation as well as in the exploration of hydrocarbons in the oil industry [14–22]. Such techniques provide the necessary information for constructing a realistic model of the geothermal system and assessing the potential of the resource. The electric resistivity is related to various geological parameters such as the mineral and fluid content, porosity and degree of water saturation in the rock [23].

A number of 2D electric profiles are performed at the location of the hot springs in Wadi Al-Lith area. The Syscal-R1 system (IRIS instruments) with 72 multi-electrodes system, with  $4 \times 18$  electrode cables is used for conducting the field surveys using different electrode spacing (1 m, 3 m, 5 m and 10 m) arranged along a

profile. Wenner-Schlumberger arrangement is used and the surveyed sections are taken very close to and crossing the hot spring. RES2DINV software is used for processing, correcting and interpretation of electric resistivity data. It can operate large datasets collected by a large number of electrodes and can account for the topographical effect along the survey lines. Finally, it generates two-dimensional resistivity model for subsurface from electrical imaging surveys [23].

### 3.3. Petro-thermal characteristics of thermal water

The petro-thermal characteristics of thermal water of Ain Al Harrah hot spring at Wadi Al-Lith area are mainly enhanced through analyzing water samples collected from the hot spring and a very close water well. These water samples are analyzed using the ICP-MS spectrometer. The analysis was performed by Perkin-Elmer Sciex instruments multi-element ICP-MS spectrometer (type ELAN9000) equipped with standard torch, cross flow nebulizer and Ni sampler and skimmer cones. Tables 1 and 2 show the chemical analyses (major, minor and trace elements) of two water



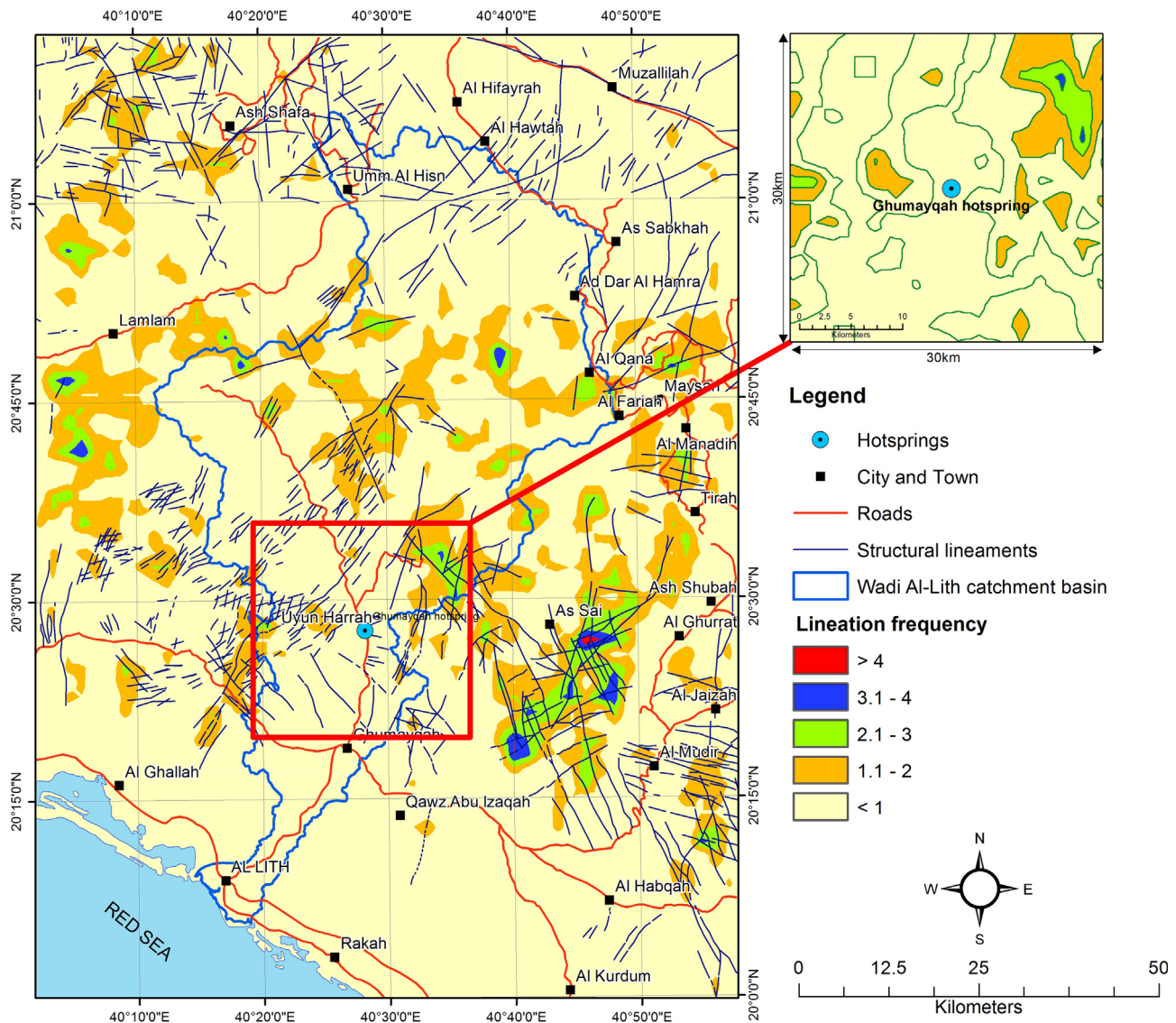


Fig. 8. Lineation frequency grid map of Wadi Al-Lith basin including Ain Al Harrah area.

samples taken from Ain Al Harrah hot spring and the neighboring water well.

### 3.3.1. Geo-thermometers

Geo-thermometer is a chemical substance or isotope in water that may be used to predict the subsurface temperature in geothermal systems. The basic assumption behind using the geo-thermometers is the chemical equilibrium between the substance (isotope) and mineral (s) in the reservoir. Theoretically, any cation ratio and any aqueous species concentration can be used as a geo-thermometer as long as equilibrium prevails. A temperature equation for a geo-thermometer is a temperature equation for a specific equilibrium constant referring to a specific mineral-solution reaction [24–29].

A selected number of geo-thermometers (Quartz, Chalcedony, Na, K, Ca geo-thermometers and combinations of them; i.e. Na–Ca and Na–K–Ca) are applied for determining the subsurface formation temperature, discharge enthalpy and heat flow. These geo-thermometers have a low to medium temperature range of 25–250 °C that fit with the thermal properties of the hot spring under

study. Eqs. (1)–(7) demonstrate the mathematical expressions of these geo-thermometers [24–29]:

#### (a) Silica geo-thermometers

##### Quartz

$$T_1(^{\circ}\text{C}) = \frac{1309}{5.19 - \log Q_z} - 273.15 \quad (\text{Range of } ^{\circ}\text{C} : 25-250) \quad (1)$$

$$T_2(^{\circ}\text{C}) = 42.198 + 0.28831Q_z - 3.6686 \times 10^{-4}Q_z^2 + 3.1665 \times 10^{-7}Q_z^3 + 77.034\log Q_z \quad (\text{Range of } ^{\circ}\text{C} : 25-250) \quad (2)$$

##### Chalcedony

$$T_1(^{\circ}\text{C}) = \frac{1032}{4.69 - \log Q_z} - 273.15 \quad (\text{Range of } ^{\circ}\text{C} : 25-250) \quad (3)$$

$$T_2(^{\circ}\text{C}) = \frac{1112}{4.91 - \log Q_z} - 273.15 \quad (\text{Range of } ^{\circ}\text{C} : 25-250) \quad (4)$$

#### (b) Na–K–Ca geo-thermometers

**Na–K**

$$T_1(^{\circ}\text{C}) = \frac{933}{0.993 + \log(\text{Na}/\text{K})} - 273.15 \quad (\text{Range of } ^{\circ}\text{C} : 25\text{--}250) \quad (5)$$

**Na–C**

$$T_1(^{\circ}\text{C}) = \frac{1096.7}{3.08 - \log(\text{Na}/\text{Ca}^{0.5})} - 273.15 \quad (\text{Range of } ^{\circ}\text{C} : 25\text{--}250) \quad (6)$$

**Na–K–Ca**

$$T_1(^{\circ}\text{C}) = \frac{1647}{\log(\text{Na}/\text{K}) + \beta \log(\text{Ca}^{0.5}/\text{Na}) + 2.24} - 273.15 \quad (\text{Range of } ^{\circ}\text{C} : 0\text{--}350) \quad (7)$$

**3.3.2. Ternary diagrams**

Three ternary (Cl–SO<sub>4</sub>–HCO<sub>3</sub> and Na+K–Ca–Mg) and Giggenbach (Na–K–Mg) diagrams are constructed for Ain Al Harrah hot spring to classify its thermal water (based on major anions and cations) and to indicate the prevailing subsurface thermal conditions [30,31].

**3.4. Geothermal reserve estimation**

Geothermal reserves are defined as quantities of thermal energy which are expected to be recovered from known reservoirs from a given date forward. The reserve is that part of the resources which could be extracted economically and legally at present and that are known and characterized by drilling or by geochemical, geophysical and geological evidence [32,33].

The most common approach for geothermal reserve estimation is the volumetric method. This method is mainly utilized in the later stages of geothermal exploration and after that in the early stages of field development to justify drilling and commitment for a specified power plant size, although may be used if good surface indications and geophysical surveys are available [34]. It can be better applied during this stage than numerical modeling which requires a significant number of wells and production history to be considered reliable [35].

In general, the reservoir parameters necessary for geothermal-reserve estimation are gathered from the analyses of the temperature data and from other geophysical and geochemical interpretations. A computer program (RESPAR, ICEBOX software)

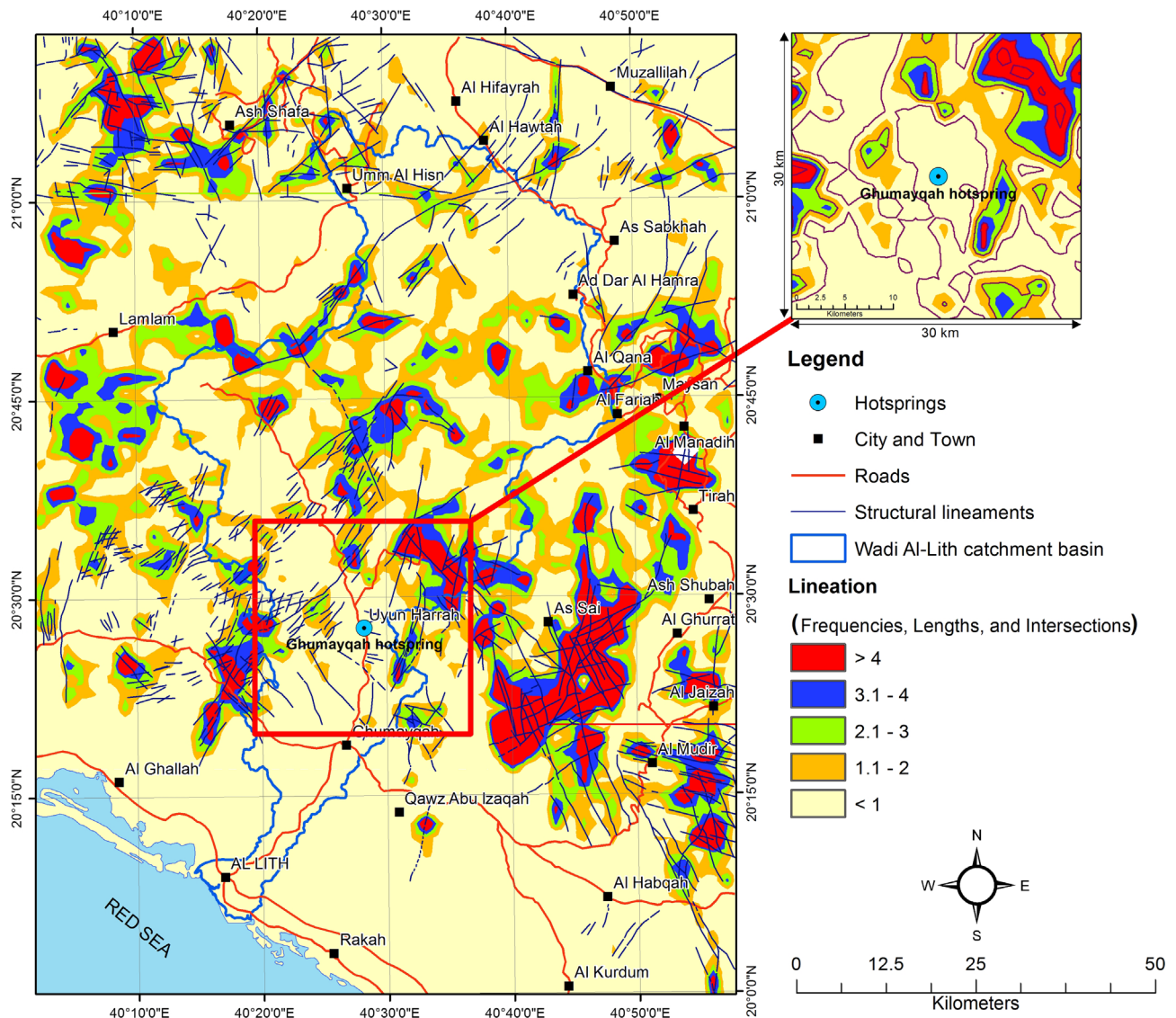


Fig. 9. Accumulation grid map of the intersection, length and frequency of the extracted lineaments of Wadi Al-Lith basin.

is used to estimate the different reservoir properties providing that the temperature, porosity and the reservoir thickness parameters are known. The total stored energy of the geothermal reservoir can be regarded as the sum of energy stored in the rock ( $E_r$ ) and the energy represented by the fluid stored in the pore spaces ( $E_f$ ). It can be estimated using the following equation:

$$E_t = E_r + E_f = V(1-\phi)\rho_r C_r (T_i - T_o) + V\phi \rho_w C_w (T_i - T_o) \quad (8)$$

Where  $E_t$  is the total thermal energy (J) in the rock ( $E_r$ ) and fluid ( $E_f$ );  $\phi$  is the reservoir porosity (%);  $V$  is the reservoir volume ( $m^3$ );  $\rho_{r,w}$  are the densities of rock and water ( $kg/m^3$ );  $C_{r,w}$  are the heat capacities of rock and water ( $J/kg^\circ C$ ) and  $T_i$ ,  $T_o$  are the initial reservoir and the reference temperatures ( $^\circ C$ ).

This stored thermal energy can be converted into power potential using the following equation:

$$\text{Power Potential (MWt)} = \frac{E_t \times RF \times CE}{PL \times LF} \quad (9)$$

where RF is the recovery factor, CE is the conversion efficiency, PL is the geothermal plant life in years and LF is the load factor.

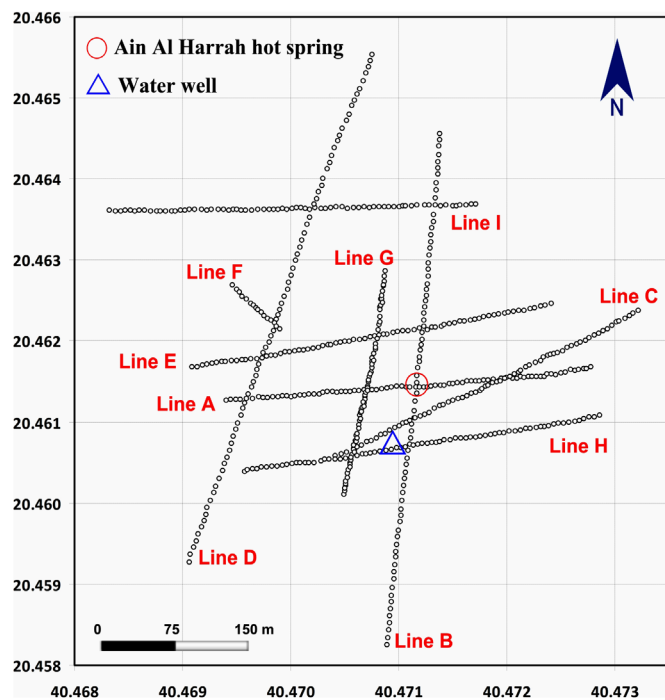


Fig. 10. Base map of Ain Al Harrah hot spring, showing the location of the 2D electric profiles.

## 4. Results and discussion

### 4.1. Lineaments extraction and analysis

The analysis of lineaments has clarified that about 10,000 elements are detected in Wadi Al-Lith basin (Fig. 4). RockWorks software is mainly utilized for drawing the rose diagram for detecting the general trends of these lineaments in Wadi Al-Lith basin and more specifically in Ain Al Harrah area (Fig. 5). The diagram illustrates that the prevailing structural elements are nearly the same and almost all lineaments are oriented and trended from  $0^\circ$  to  $90^\circ$  (or  $180^\circ$ – $270^\circ$ ) with mean trend vector of  $33^\circ$  (or  $213^\circ$ ). Few lineaments are oriented along a northwest–southeast direction in Ain Al Harrah hot spring area (Fig. 5b). Tables 3 and 4 summarize the main structural trends of these lineaments, as well as their percent, lengths and frequency.

Figs. 6–8 show the constructed intersection, length and frequency property maps for all the extracted lineaments in Wadi Al-Lith area. An accumulation grid map for these three properties is drawn, to illustrate their combined effect (Fig. 9). This map shows how much these three components behave and affect the study area. The weighting factor or influence of each component in the accumulation grid map was chosen to be, lineation intersection (3), lineation length (2) and lineation frequency (1).

Interpretation of these figures shows that, no more than three lineament elements are acting together in the study area. This assigns middle to low influence of these elements in Wadi Al-Lith catchment area. Outside Wadi Al-Lith area, on the other hand, a high combined influence of these structural lineaments is recorded in the order of four elements (Fig. 9). The result that can be concluded from this lineament analysis is that the surface structural elements are not the factor that control the movement of the deep arising thermal water of the main hot spring in Wadi Al-Lith area, and that there might be another subsurface elements that could carry out this geothermal water to the surface.

### 4.2. Interpretation of geophysical profiles

Out of the nine conducted 2D electric resistivity sections, three are selected to demonstrate the prevailing structural elements. These profiles are specifically conducted in the area of the hot spring (Fig. 10). The results obtained from these profiles are mainly concerned with the pathways of geothermal water, detecting feed zones, the influencing structural elements and the possible failure system.

Fig. 11 exhibits the interpreted 2D electric section (Line I) that is extended along an east–west direction. It shows a tilted thermal feed zone at the middle of the section oriented along a very obvious fault zone. The strike of this fault is found to be along a northwest–southeast direction which is considered the main prevailing structure in the area (Red Sea Rift). This structure trend

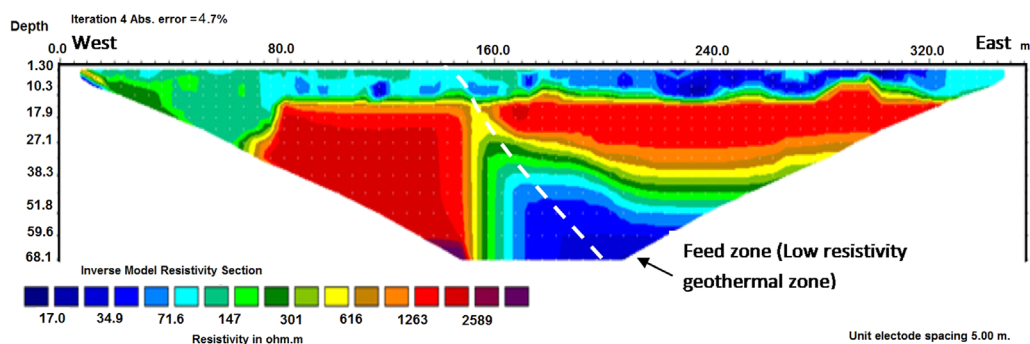


Fig. 11. 2D interpreted resistivity profile (line I) extending East–West, Wadi Al-Lith area.



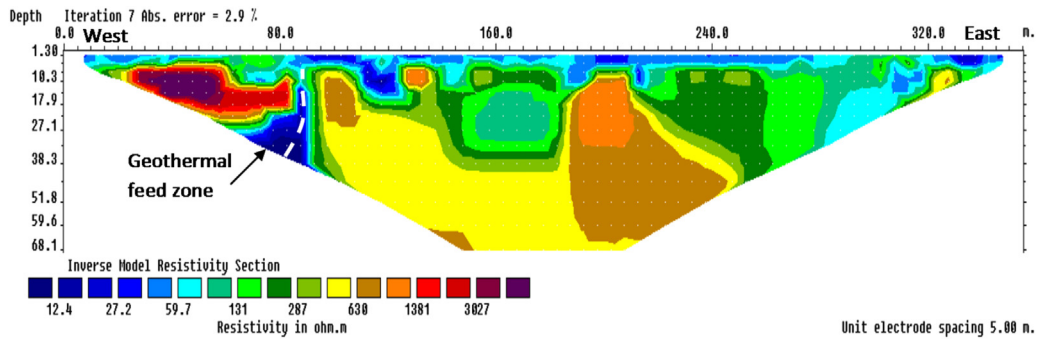


Fig. 12. 2D interpreted resistivity profile (line H) extending East–West, Wadi Al-Lith area.

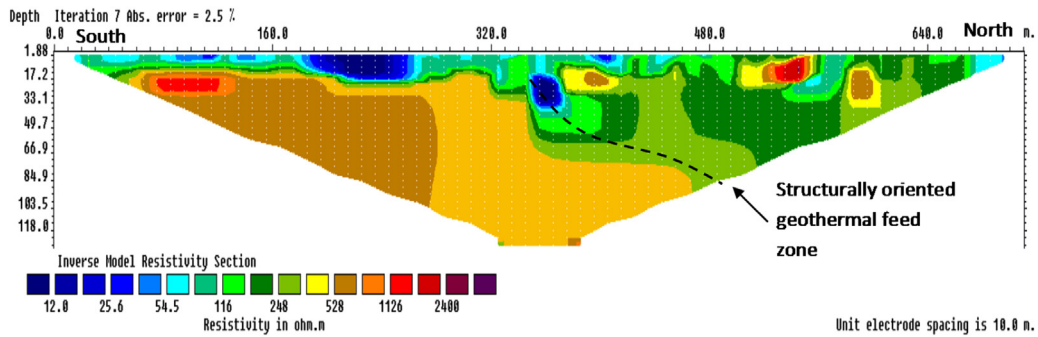


Fig. 13. 2D interpreted resistivity profile (line B) extending North–South, Wadi Al-Lith area.

Table 5

Petro-thermal parameters of Ain Al Harrah hot spring, Wadi Al-Lith area.

Hot spring	Subsurface temp. (°C)	Discharge enthalpy (kJ/kg)	Heat flow (mW/M <sup>2</sup> )
Ain Al Harrah	136	219	183

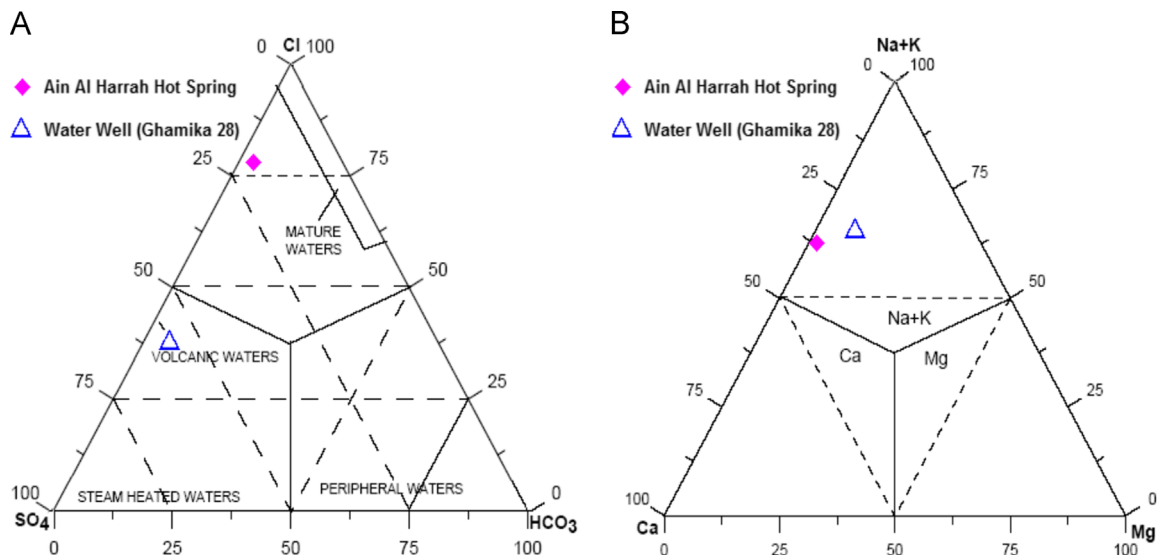


Fig. 14. Type of thermal fluids of Ain Al Harrah hot spring as inferred from; (A) Cl–SO<sub>4</sub>–HCO<sub>3</sub> and (B) Na+K–Ca–Mg ternary diagrams.

is opposite to another oriented northeast–southwest geothermal feed zone, detected at the western end of the profile H between electrodes 80–90 (Fig. 12).

Fig. 13, on the other hand, represents another 2D electric profile extending from north to south (Line B). A suggested fault system is recognized at the middle of the section. This may be interpreted as a

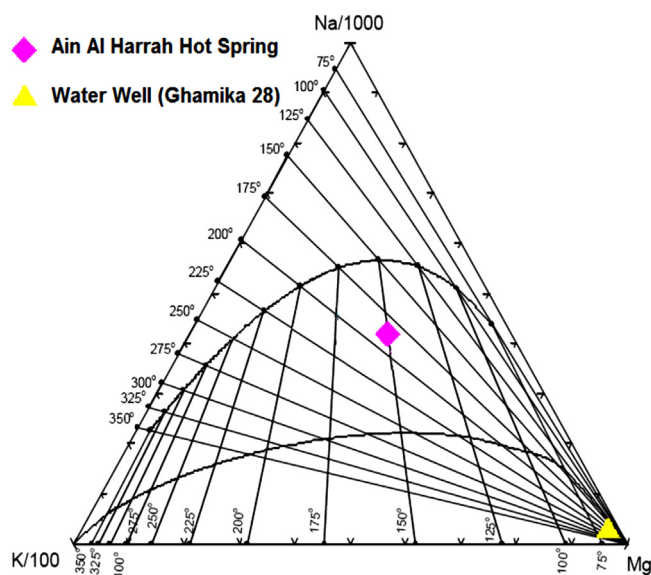


Fig. 15. Giggenbach diagram of Ain Al Harrah hot spring, Wadi Al-Lith area.

result of the well known northeast–southwest trending faults that influence the western coastal parts of the Red Sea area. In general, the feed zones of thermal waters are indicated by lower resistivity values and the structural control of the thermal water is obvious.

#### 4.3. Characteristics of thermal water

The petro-thermal parameters which are indicated from the geo-thermometers are listed in Table 5. It appears clearly that the Ain Al Harrah hot spring attains good and high geothermal parameters. The weighted values of the estimated subsurface formation temperature, discharge enthalpy and heat flow are found to be 136 °C, 219 kJ/kg and 183 mW/M<sup>2</sup>, respectively.

Figs. 14 and 15 represent the constructed ternary (Cl–SO<sub>4</sub>–HCO<sub>3</sub> and Na+K–Ca–Mg) and Giggenbach (Na–K–Mg) diagrams for Ain Al Harrah hot spring and one neighboring water well. These diagrams are used to indicate the type of the geothermal water and the subsurface geothermal condition at which the dissolved ions of the surface ascending thermal fluids are originated.

The ternary diagrams illustrate that the water type of the hot spring is completely different than that of the neighboring water wells. The increase of the concentration of the chlorine anion (mg/l) on the expanse of the sulfate and carbonate anions is very clear on the hot spring (Fig. 14a). On the other hand, a considerable increase of the Mg cation is indicated for the water well sample on the expanse of the Na+K and Ca cations (Fig. 14b). A mature water type, most probably mixed with surface water is indicated to the hot spring, while a volcanic unmixed water type is given for the water well. Giggenbach (Na–K–Mg) diagram shows that Ain Al Harrah hot spring assigns higher geothermal parameters than the water well. The cluster of this hot spring is located along the 150 °C Mg–K and the 175 °C–225 °C Na–K iso-thermal lines, while that of the water well is located very close to the Mg corner along iso-thermal lines of less than 50 °C assuming very low geothermal regime (Fig. 15).

Another unique difference in water type, is the increase of the concentration of some radioactive elements in the hot spring like rubidium (Rb, 68.9 ppm) and strontium (Sr, 4160 ppm) more than those in the water well (Rb, 0.587 ppm and Sr, 4160 ppm).

#### 4.4. Geothermal energy potential

In this study, geothermal-reserve estimation is carried out for evaluating the possible geothermal capacities of Ain Al Harrah hot

Table 6

Reservoir parameters used for geothermal reserve estimation.

Property		Unit	Value
Reservoir	Volume	km <sup>3</sup>	1.28
	Porosity	%	4
Density	Rock	kg/m <sup>3</sup>	2800
	Water	kg/m <sup>3</sup>	980
Heat capacity	Rock	J/kg °C	1000
	Water	J/kg °C	4200
Temperature	Initial	°C	95
	Reference	°C	45

spring. Reserve estimation is based on the above mentioned Eqs. (8) and (9), assuming the following parameters:

- A reservoir area of 4.8 km<sup>2</sup> (1.2 × 4.0 km<sup>2</sup>) and reservoir volume of 1.28 km<sup>3</sup> providing a reservoir thickness of 250 m as concluded from the interpretation of resistivity data.
- An initial temperature of 95 °C for the geothermal reservoir.
- A reference temperature of 45 °C is suggested (due to the higher average annual surface temperature in Saudi Arabia).
- Pore volume range of 3–5 p.u. for the fractured granitic rocks (average value of 4 p.u.).
- Density range of 2.7–2.90 g/cc (average value of 2.80 g/cc).

The different reservoir parameters that are derived from the analyses of temperature and geo-thermometer data and can be used in thermal energy estimation are represented in Table 6. According to these parameters and by applying in Eq. (8), the total stored heat energy of Ain Al Harrah geothermal area is found to be 1.713 × 10<sup>17</sup> J (1.34 × 10<sup>16</sup> J for thermal fluids and 1.57 × 10<sup>17</sup> J for reservoir rock).

The total stored heat energy of Ain Al Harrah hot spring can be converted into power energy units (megawatt thermal using Eq. (9)) for possible energy production and other low geothermal utilizations. Assuming recovery factor of 0.2 (normal factor for geothermal reservoirs), turbine conversion efficiency of 0.47, (initial temperature/reservoir temperature) plant life of 20 years and load factor of 0.95, the thermal power potential of Ain Al Harrah geothermal reservoir is found to be 26.99 MWt. This geothermal reserve is considered a very promised and can be used for providing the Al Lith area with electricity (clean energy) on a long term basis. We strongly recommend exploiting this geothermal system to generate electricity for the first time in Saudi Arabia using a specific power plant that operates thermal fluid that boils at low temperature (e.g. Kalina Cycle).

##### 4.4.1. Utilization of geothermal energy in Saudi Arabia and economic and social impact

The estimated geothermal energy ( MWt) is quite enough for possible electricity production in Saudi Arabia. Kalina power plants can be used due to the lower boiling point (70 °C) of their fluids. Having a higher temperature range than the boiling point of the Kalina cycle, the thermal water of Ain Al Harrah hot springs can be economically used for power generation. However, this thermal water can be utilized directly in other low forms of applications (district heating, fish farming, agricultural applications, greenhouses, etc.). Some of these applications are already now in use (Gouba area, central Saudi Arabia), where a number of geothermal-based natural therapy, medical and swimming pools are constructed.

The social factor of using the geothermal energy implies from the fact that most of the geothermal resources are mainly located in the extreme western and south-western borders of Saudi Arabia along the coast of the Red Sea. These areas besides being far are

topographically complicated, not so easy to reach and need more developments in its infrastructures and the level of the residence Bedouins people. The geothermal based-energy can help in constructing new modern communities fed with the geothermal-based energy, where no high voltage transmission lines are available in the vicinity and where it would be too expensive to connect to the national electric grid.

## 5. Conclusions

The following conclusions may be drawn according to the present study:

1. Wadi Al-Lith area contains one of the most promised geothermal systems in the western of Saudi Arabia. It is located near the coast of the Red Sea and is strongly affected by its tectonic activity and structural regimes.
2. Ain Al Harrah hot spring is considered the main geothermal target in Wadi Al-Lith area that attains high surface temperature upto 95 °C and good petro-thermal characteristics of 136 °C (reservoir temperature), 219 kJ/kg (discharge enthalpy) and 183 mW/M<sup>2</sup> (heat flow) as indicated from the geothermometric analysis.
3. The analysis of Landsat RGB images (lineaments extraction) and the interpretation of the electric geophysical profiles have clarified the presence of many surface and subsurface structural elements. Feed zones of thermal waters are indicated by lower resistivity values and the structural control of the thermal water is obvious. Majority of the encountered geothermal feed zones are tilted and aligned along a north-east–southwest (transform) direction and little bit to a north-west–southeast one (Red Sea Rift).
4. Almost all surface structural lineaments that control the movement of the geothermal water (Ain Al Harrah hot spring) are found following the main structural trends of Wadi Al-Lith area.
5. The analysis of ternary and Giggenbach diagrams shows that the water type of geothermal system is completely different than the neighboring domestic water aquifers. A mature mixed water type is assigned for Ain Al Harrah hot, while a volcanic unmixed water model is given for the neighboring water wells.
6. The stored heat energy is found to be  $1.34 \times 10^{16}$  J for the thermal fluids and  $1.57 \times 10^{17}$  J for the hot rock.
7. A geothermal power potential of 26.99 MWt is estimated for Ain Al Harrah hot spring which is considered good and adequate for economic investment.
8. A medium scale power plant that utilizes fluids of low boiling point is recommended for possible electricity generation for the first time in Saudi Arabia.
9. A very strong and positive economic-social impact will be obtained upon applying such geothermal technology in the study area or in other remote areas of similar geothermal systems. It will enhance the infrastructure and build up a new geothermal-feed communities based on clean renewable energy.

## Acknowledgments

This work is funded and supported by the National Plan for Science, Technology and Innovation program (NPST)—King Saud University, project number 10-ENE1043-02. Part of work is also supported by the Saudi Geological Survey through the M. Sc. of Ibrahim Al Zahrani. The authors would like to pay an attribute of

their college Prof. Dr. Mohamed Tahir Hussein who passed away during the period of the preparation of this publication. Prof. Hussein contributed to this work and we find ourselves obliged to include his name among the authors.

## References

- [1] Renewables. Global status report; 2011, p. 17–18.
- [2] Lashin A, Shata A. An analysis of wind power potential in Port Said, Egypt. *Renewable and Sustainable Energy Reviews* 2012;16:6660–7.
- [3] Stefansson V. The renewability of geothermal energy. In: *Proceedings of the world geothermal congress, Kyushu (Japan)*; 28 May–10 June 2000, CD-ROM.
- [4] Glassley W. *Geothermal energy: renewable energy and the environment*. Boca Raton, 290p: CRC Press; 2010.
- [5] Geothermal energy association. *Geothermal energy: international market update*; May 2010. p. 4–6.
- [6] Comps J, Muffler LJP. Exploration for geothermal resources. In: Kruger P, Otte C, editors. *Geothermal energy—resources, production, stimulation*. Stanford: Stanford University Press; 1973. p. 95–128.
- [7] Al Dayel M. Geothermal resources in Saudi Arabia. *Geothermics* 1988;17(2/3):465–76.
- [8] Lashin A, Al Arifi N. The geothermal potential of Jizan area, Southwestern parts of Saudi Arabia. *International Journal of Physical Sciences* 2012;4:664–75.
- [9] Roobol MJ, Camp VE. Geologic map of the Cenozoic lava field of Harrats Khaybar, Ithnayn, and Kura, Kingdom of Saudi Arabia. Saudi Directorate General of Mineral Resources Geoscience Map GM-131, with explanatory text.60.
- [10] Roobol MJ, Camp VE. Geologic map of the Cenozoic lava field of Harrat Kishb. Kingdom of Saudi Arabia: Saudi Arabian Directorate General of Mineral Resources Geoscience Map GM-132, with explanatory text.34.
- [11] Roobol MJ, Bankher K, Bamufleh S. Geothermal anomalies along the MMN Volcanic Line including the cities of Al Madinah al Munawwarah and Makkah al Mukarramah. Saudi Arabian Deputy Ministry for Mineral Resources Confidential Report DMMR-MADINAH-CR-15-2.95.
- [12] Pint J. Master list of GPS coordinates for Saudi Arabia caves. Saudi Geological Survey Confidential Data File SGS-CDF-2001-1.
- [13] Pint J, Al Shanti M, Al Amoudi S, Hibashi Forti P, GharAl. Harrat Nawasif/Al Bukim, Kingdom Saudi Arabia. Open-File Report, Saudi Geological Survey.74.
- [14] Pint J. Prospects for lava-cave studies in Harrat Khaybar, Saudi Arabia. Saudi geological survey; 2006.
- [15] Abd El Naby A, Abd El-Aal M, Kuss J, Boukharay M, Lashin A. Structural and basin evolution in Miocene time, Southwestern Gulf of Suez, Egypt. *Neues Jahrbuch für Geologie und Paläontologie—Abhandlungen (Germany)*, 251; 331–353.
- [16] Lashin A, Al-Arifi N, Abu Ashour N. Evaluation of the ASL and Hawara formations using seismic- and log-derived properties, October Oil Field, Gulf of Suez, Egypt. *Arabian Journal of Geosciences* 2011;3–4:365–83.
- [17] Al-Arifi N, Lashin A, Al-Humidan S. Migration of local earthquakes in the Gulf of Aqaba, Saudi Arabia. *Earth Science Research* 2012;16(1):35–40.
- [18] Lashin A, Ahmed G, Abd El Aal M. Improving and predicting the petrophysical parameters of the reservoirs using Monte Carlo simulation and stochastic analysis. *Journal Egyptian Geophysical Society* 2006;4(1):1–16.
- [19] Lashin A, Serag Al Din S. Reservoir parameters determination using artificial neural networks: Ras Fanar field, Gulf of Suez, Egypt. *Arabian Journal of Geosciences* 2012. <http://dx.doi.org/10.1007/s12517-012-0541-6>, 18p.
- [20] Lashin A. Reservoir parameter estimation using well logging data and production history of the Kalderholt geothermal field, S-Iceland. Iceland: UNU-GTP; 12.
- [21] Lashin A. Evaluation of the geothermal potential around the coastal parts of the Gulf of Suez, Egypt, using well logging and the geo-thermometer data. *Journal of Applied Geophysics* 2007;6(2):215–48.
- [22] Lashin A. A preliminary study on the potential of the geothermal resources around the Gulf of Suez, Egypt. *Arabian Journal of Geosciences* 2012, 10.1007/s12517-012-0543-4, 22p.
- [23] Loke MH. *Electrical imaging surveys for environmental and engineering studies: a practical guide to 2-D and 3-D surveys*. 11700 Penang, Malaysia: Minden Heights; 57.
- [24] Fournier RO, Rowe JJ. Estimation of underground temperatures from the silica content of water from hot springs and wet-steam wells. *American Journal of Science* 1966;264:685–97.
- [25] Fournier RO. Estimating the subsurface formation temperature of the geothermal reservoirs using the soluble chalcedony. *Geothermics* 1977;5:41–50.
- [26] Fournier RO, Potter A. Using of quartz geo-thermometer as indicator for subsurface temperatures. *Bulletin Geothermal Resources Council* 1982;3–12.
- [27] Arnorsson S. The use of mixing models and chemical geo-thermometers for estimating underground temperatures in geothermal systems. *Journal of Volcanological and Geothermal Research* 1985;23:299–335.
- [28] Arnorsson S. Isotopic and chemical techniques in geothermal exploration, development and use: sampling methods, data handling and interpretation. Introductory course. IS-108 Reykjavik, Iceland: GTP; 199.
- [29] Arnorsson S, Gunnarson I, Stefansson A, Andresdottir A, Sveinbjornsdottir AE. Major element chemistry of surface and ground waters in basaltic terrain N-Iceland. *Geochimica et Cosmochimica Acta* 2002;66:4015–46.



- [30] Giggenbach, WF. Graphical techniques for the evaluation of water–rock interaction conditions by use of Na, K, Mg and Ca contents of discharge waters. In: Proceeding of the 8th New Zealand Geothermal Workshop; 1986. p. 37–44.
- [31] Giggenbach WF. Geothermal solute equilibria derivation of Na–K–Mg–Ca geoindicators. *Geochimica et Cosmochimica Acta* 1988;52:2749–65.
- [32] Muffler P, Cataldi R. Methods for regional assessment of geothermal resources. *Geothermics* 1978;7:53–89.
- [33] Dickson MH, Fanelli M. What is geothermal energy. Internal report. Pisa, Italy: Istituto di Geoscienze e Georisorse, CNR; 61.
- [34] Clotworthy AW, Ussher GNH, Lawlessl JV, Randle JB. Towards an industry for geothermal reserves determination. *GRC Transactions* 2006;30, 9p.
- [35] Sarmiento ZF, Steingrimsson B. Computer program for resource assessment and risk evaluation using Monte Carlo simulation. Short course on geothermal project management and development. Entebbe, Uganda: UNU-GTP, KenGen and MEMD-DGSM; 2008.